

## MODIS Case 2 Ocean Color Algorithms: Use of MODIS SST to Condition the Bio-optical Domains via Nitrate-Depletion Temperatures

By

K. Carder, R. Chen, J. Patch, and J. Brown

The chlorophyll-specific absorption coefficient at 443 nm,  $a_{(443)}$ , of phytoplankton-rich particles in the ocean can change on a global basis by a factor of 8 to 10 (e.g. see Bricaud et al. 1995), making extremely difficult any accurate conversion from absorption coefficients (optical properties actually determined with MODIS) to chlorophyll *a* concentrations, [Chl *a*]. MODIS team objectives are to determine chlorophyll *a* values to better than 35% (Esaias et al. 1998), a significant task. It is only because many phytoplankton optical properties co-vary with [chl *a*] that historical pigment algorithms retrieve values within 50-100% (see O'Reilly et al 1998). For waters rich in colored dissolved organic matter, CDOM, however, or those with low pigment concentrations at high latitudes, even these co-variations disappear, requiring algorithms that distinguish between pigments and CDOM and adjust for variations in  $a_{(\lambda)}$  through an independent variable (Carder et al. 1999).

The nitrate-depletion temperature (NDT) for a given oceanic location is the temperature above which the nitrate concentration becomes negligible (Kamykowski 1987). It is indicative of a place where a major transition is occurring in the types of phytoplankton that can successfully compete for resources. Comparing the sea-surface temperature (SST; Fig. 1) to the nitrate-depletion temperature (Fig. 2) provides a means of estimating nutrient availability and allows partitioning into bio-optical domains (Fig. 3), each with much smaller ranges of  $a_{(\lambda)}$  (Carder et al. 1999). This allows the ratio of chlorophyll *a* to accessory pigments and cell optical size to change with bio-optical domain (e.g. summer versus spring in the Sargasso Sea; Bissett et al. 1999 a, b) and hence the particle absorption determined from MODIS to be more accurately interpreted in terms of chlorophyll *a* concentration. A transect from the Sargasso Sea in late spring across the Gulf Stream toward the Gulf of Maine provides a change of than 10° C within less than 30 km (Fig. 1), suggesting dramatic bio-optical changes in just a short distance.

Operationally, the MODIS chlorophyll *a* algorithm (MOD\_chl\_a\_3), released by the MODIS data archive (DAAC) in November 2000, uses weekly averaged SST values (Reynolds and Smith 1994), which were composited into 1° x 1° bins prior to availability of calibrated MODIS SST values. The low temporal and spatial resolution of these composites, however, caused switches between bio-optical domains to occur at locations that were not always regions of thermal gradients, implanting artificial steps in otherwise uniform chlorophyll fields (Fig. 4). While seasonal changes away from the edges of large biomes are more likely to be properly expressed with the low-resolution Reynolds SST values, transitional regions, such as those represented in Figure 1, require high-resolution synoptic SST data.

Implementation of MODIS-derived SST values for use in selection of bio-optical domains removes the effects of mismatched temporal and spatial scales between the SST and radiance fields, providing synoptic domain selection on a pixel-by-pixel basis. Developing a smooth transition rather than step-wise algorithm switches across bio-optical boundaries (Fig. 5) also mitigates striping effects due to minor inconsistencies in calibration and round-off errors among each of the 10 detector elements per band that simultaneously and contiguously view a given nominal 10-km swath of the ocean. Adjacent 10-pixel swaths at times are inconsistent due to calibration difficulties between different mirror sides, and the effects are evidenced in retrievals dependent upon the thermal channels (Fig. 1) or the short-wave visible channels (Fig. 6). These problems are continuing to be addressed in the calibration and validation activities by the MODIS team, but smoothing the transitions between bio-optical domains (Fig. 5) mitigates much of the effect on the chlorophyll fields as shown below.

This contribution provides a step-wise demonstration of the improvements made to the semi-analytical Case 2 chlorophyll algorithm for a region and time of year when gradients are maximal in thermal and bio-optical fields. The changes in algorithm performance are striking, especially when compared with results from the same algorithm locked in a single bio-optical domain with global packaging parameters for parameterization of the bio-optical model. The transition from a one-domain (Fig. 7) to a four-domain model (Fig. 8) is amazing, with lower chlorophyll values in the Gulf Stream and higher values in the Gulf of Maine for the four-domain approach. The improvements using MODIS (Fig. 8) versus Reynolds and Smith SST values (Fig. 4) are also clear, with crisp transitions at appropriate places, a wider dynamic range of chlorophyll values, and a reduction banding effects when smooth transitions between bio-optical domains are implemented.

While field values of chlorophyll *a* for May 2000 have not yet reached the major data archives, values for May in 1997-1999 for the region north of the Gulf Stream are in the 2 to 8 mg/m<sup>3</sup> range, consistent with Chl\_a\_3 values shown in Figure 8. Note that more-traditional algorithms (Chlor\_modis) produce unreasonably high chlorophyll values (> 30 mg/m<sup>3</sup>, Fig. 9) for the high-gelbstoff regions (see Fig. 6). Furthermore, values in the Gulf Stream are not low enough (note the change in the scale of the color bar).

The bio-optical domains developed using the nitrate-depletion temperature approach should also be useful in designating regimes where various species and quantum efficiencies for photosynthesis prevail. These domains could be augmented using with silica-depletion temperatures (Kamykowski 1987) to define where silica would be limiting the growth of diatoms and with phosphate-depletion temperatures to determine where phosphorus would limit the growth of nitrogen-fixing, autotrophic bacteria. These bacteria also have a higher demand for iron than other phytoplankton because of their need for making nitrogenase to fix nitrogen. Thus riverine and aeolian sources of iron also need to be considered in calculating phytoplankton growth rates and resource competition within the marine food web (Lenes et al., accepted).

The MODIS code is being updated to provide results consistent with the prototypical results shown above. Changes include a pixel-by-pixel domain selection using MODIS SST values and a linear smoothing function implemented to provide for transitions between bio-optical domains (Fig. 5). This includes an additional hyper-packaged domain to address high-latitude phytoplankton regimes such as encountered by Mitchell and Hansen (1991) near the Antarctic. The thermal contrast in the scene is caused by the warm Gulf Stream with tiny, subtropical phytoplankton juxtaposed with the cold Labrador Current with large, diatom-rich assemblages. Ice-bergs are still prevalent in May in the Labrador Current, which feeds into the region north of the Gulf Stream, and it is a region of fairly high gelbstoff (Walsh et al. 1992). Rivers also provide nutrients to the coastal waters of the region, gelbstoff, and diatoms, requiring an algorithm that separates phytoplankton absorption spectra from gelbstoff spectra, and characterizes the phytoplankton absorption in terms of chlorophyll *a* concentration through an adaptable chlorophyll-specific absorption coefficient. The Chl\_a\_3 algorithm does this, while others do not.

The absorption coefficient at 400 nm due to gelbstoff ( $a_g[400]$ ) (Fig. 6) is more sensitive to striping than is Chl\_a\_3 as it is more dependent upon the stripe-rich 412 nm channel of  $L_w$ . While not too severe on the right-hand sides of imagery,  $L_w$  values at 412 and 443 nm are especially sensitive to striping on the left-hand sides of images (e.g. Fig. 10). Until calibration consistency is achieved among the 10 elements and two mirror sides of Terra, the ability to separate the effects due to gelbstoff from those due to phytoplankton using the 412 and 443 nm channels will be severely limited. Over-estimates of chlorophyll *a* by as much as 5-fold for gelbstoff-rich, spring, high-latitude waters will not be unusual if we are forced to use only the longer-wavelength (> 443 nm) channels because of the striping problems of Terra.

#### References:

- Bissett, W. P., K.L. Carder, J.J. Walsh, D.A. Dieterle, 1999. Carbon cycling in the upper waters of the Sargasso Sea: II. Numerical simulation of apparent and inherent optical properties, *Deep-Sea Res. I* 46: 271-317.
- Bricaud, A., N. Babin, and A. Morel, 1995. Variability in the chlorophyll-specific absorption coefficients of natural phytoplankton: Analysis and parameterization. *J. Geophys. Res.* 100(C7):13321-13332.
- Carder, K.L., F.R. Chen, Z.P. Lee, and S.K. Hawes, 1999. Semianalytic Moderate-Resolution Imaging Spectrometer algorithms for chlorophyll *a* and absorption with bio-optical domains based on nitrate-depletion temperatures, *J. Geophys. Res.* 104(C3):5403-5421.
- Kamykowski, D., 1987. A preliminary biophysical model of the relationship between temperature and plant nutrients in the upper ocean, *Deep-Sea Res., Part A*, 34: 1067-1079.
- Lenes, J.M., B.P. Darrow, C. Cattrall, C.A. Heil, M. Callahan, G.A. Vargo, R.H. Byrne, J.M. Prospero, D.E. Bates, K.A. Fanning and J.J. Walsh, accepted. Iron fertilization and the *Trichodesmium* response on the West Florida shelf, *Limnol. and Oceanogr.*

- O'Reilly, J.E., S. Moritorena, B.G. Mitchell, D.A. Siegel, K.L. Carder, S.A. Garver, M.Kahru, and C. McClain, 1998. Ocean color algorithms for SeaWifs, *J. Geophys. Res.* 103: 24,937-24,953.
- Reynolds, R.W. and T.M. Smith, 1994. Improved global sea-surface temperature analysis using optimum interpolation, *J. Climate* 7:929-948.
- Walsh, J.J., K.L. Carder and F.E. Muller-Karger, 1992. meridional fluxes of dissolved organic matter in the North Atlantic Ocean. *J. Geophys. Res.* 97(C10): 15,625-15,637.

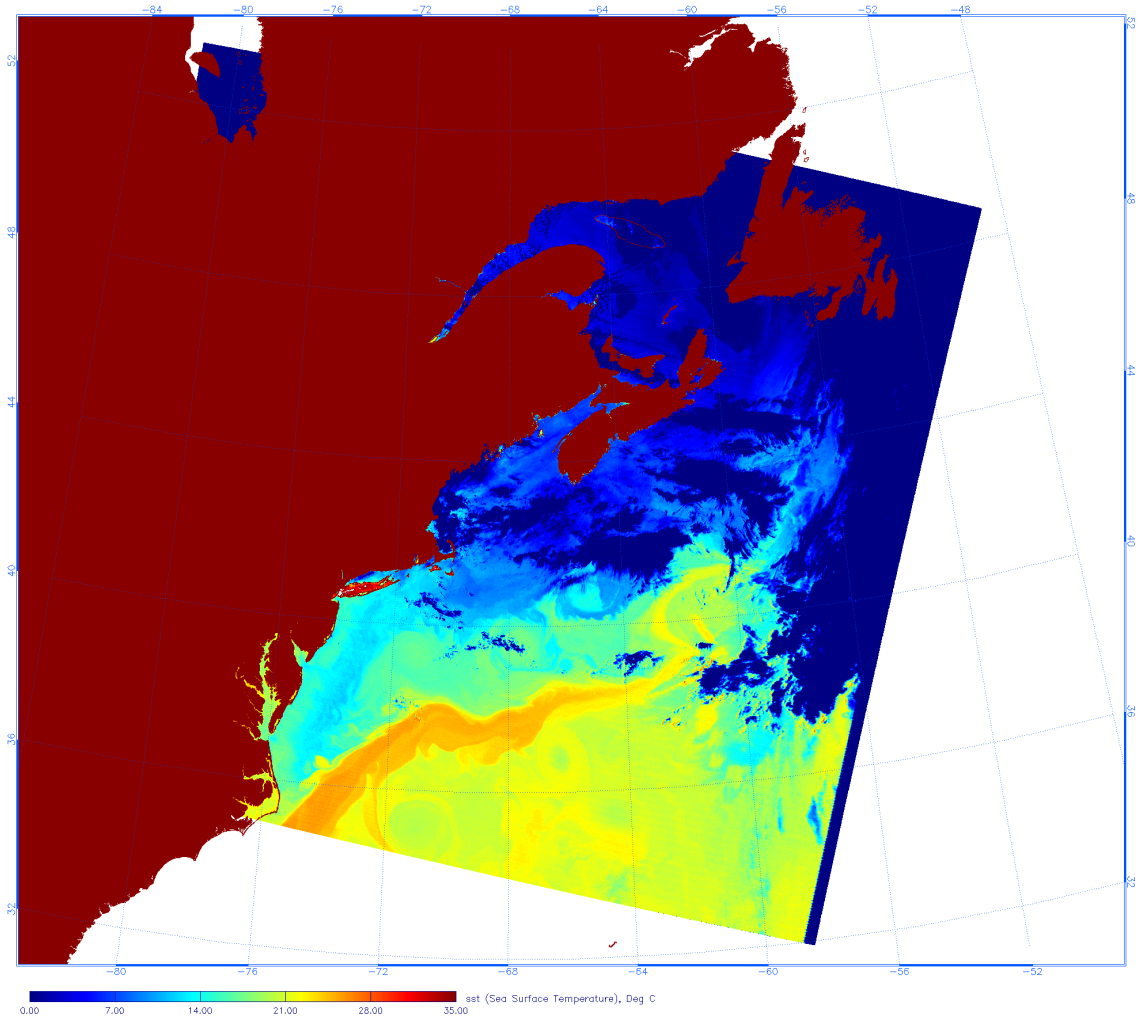


**Figure 1 Sea-surface temperature (SST) retrieved from MODIS for Julian Day JD129, 2000.**

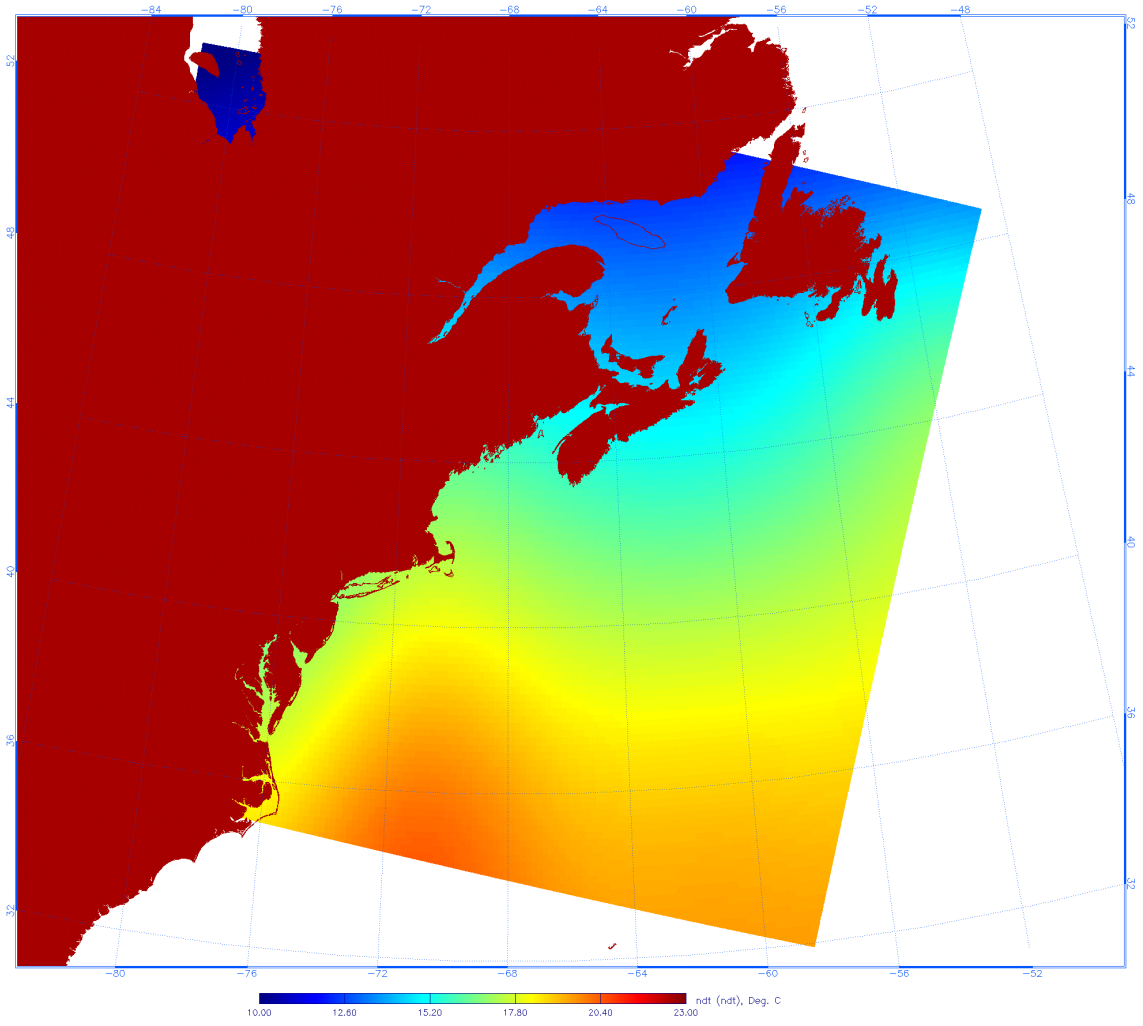


**Figure 2 Nitrate-depletion temperature (NDT) variation for the study area.**

**Figure 3 Bio-optical domains for JD129 from MODIS SST-NDT values sorted as shown in Fig. 5.**

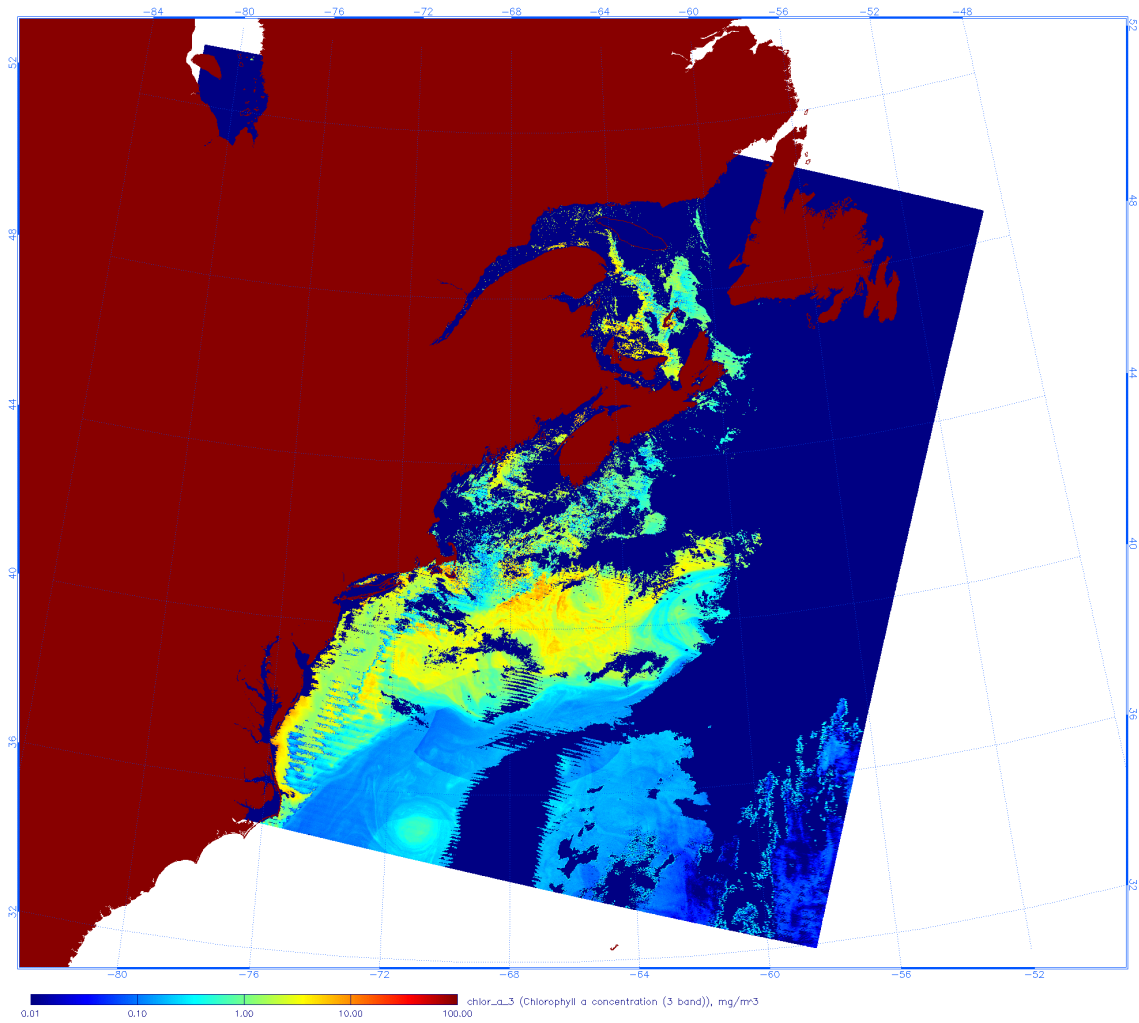


**Figure 4** Chlorophyll *a* concentrations derived using the Carder et al. (1999) algorithm with MODIS water-leaving radiances, but Reynolds and Smith (1994) weekly-composited ( $1^\circ \times 1^\circ$ ) SST values were used for selecting bio-optical domains. Note the odd chlorophyll gradient in the Gulf Stream, the non-circular cold-core eddy, and the step-gradient parallel to but north of the north wall of the Gulf Stream resulting from coarse-resolution and one-week composited of SST data.

Title  
Graphics produced by IDL  
Creator  
IDL Version 5.3 (RFX mpset)  
Preview  
This EPS picture was not saved  
with a preview window  
Comment  
This EPS picture is a  
PostScript printer, but not  
of other types of printers.

**Figure 5** Sorting schematic for bio-optical domains using SST-NDT: pk0 = global; pk1 = unpackaged; pk2 = packaged; and pk3 = hyper-packaged. Once the domains are established, the transitions between domains result from mixing of derived chlorophyll values for each domain weighted according to the dotted gradient lines.

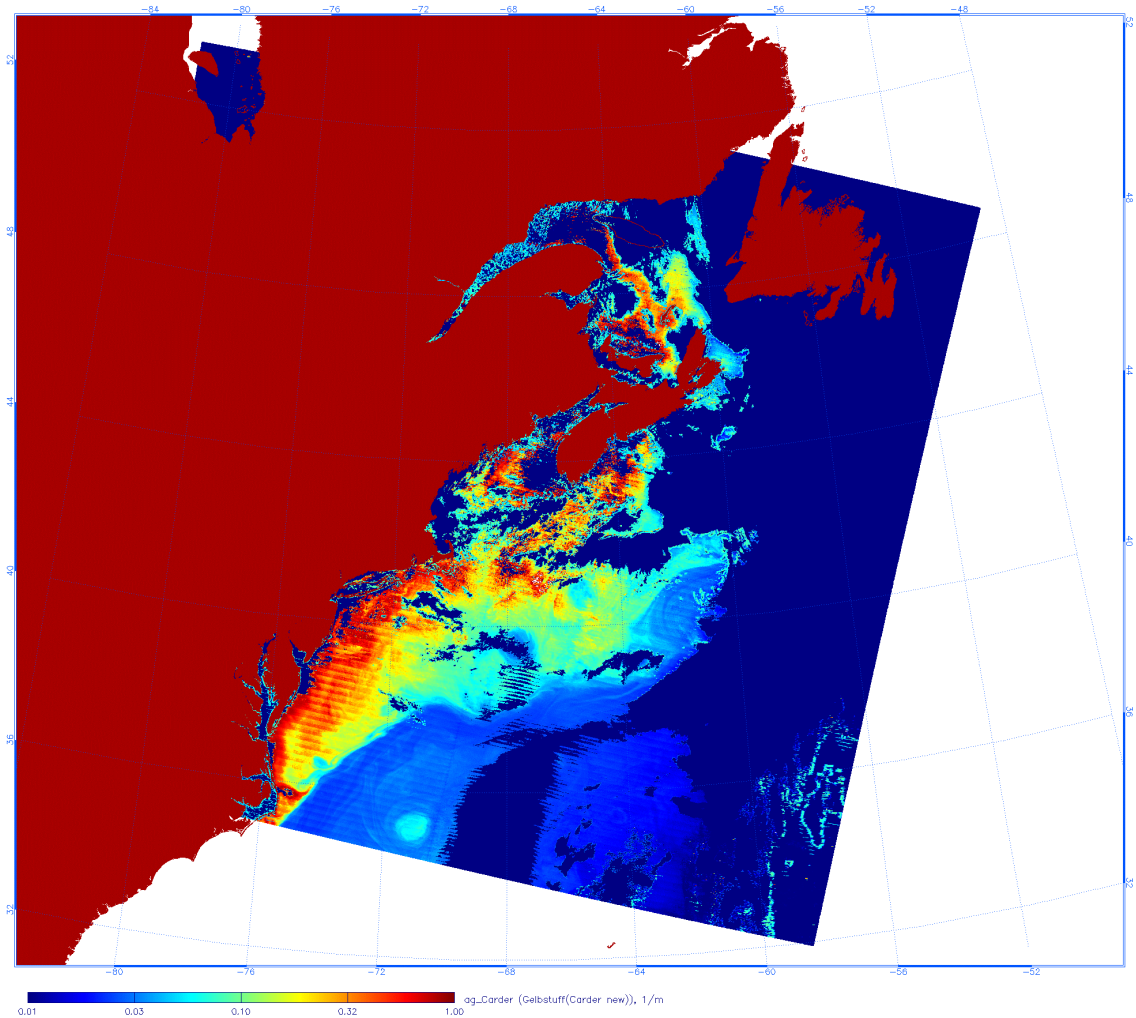


**Figure 6 Absorption coefficient due to gelbstoff at 400 nm. This algorithm is especially dependent on good calibration of the 412 nm and 443 nm channels (see Carder et al. 1999).**

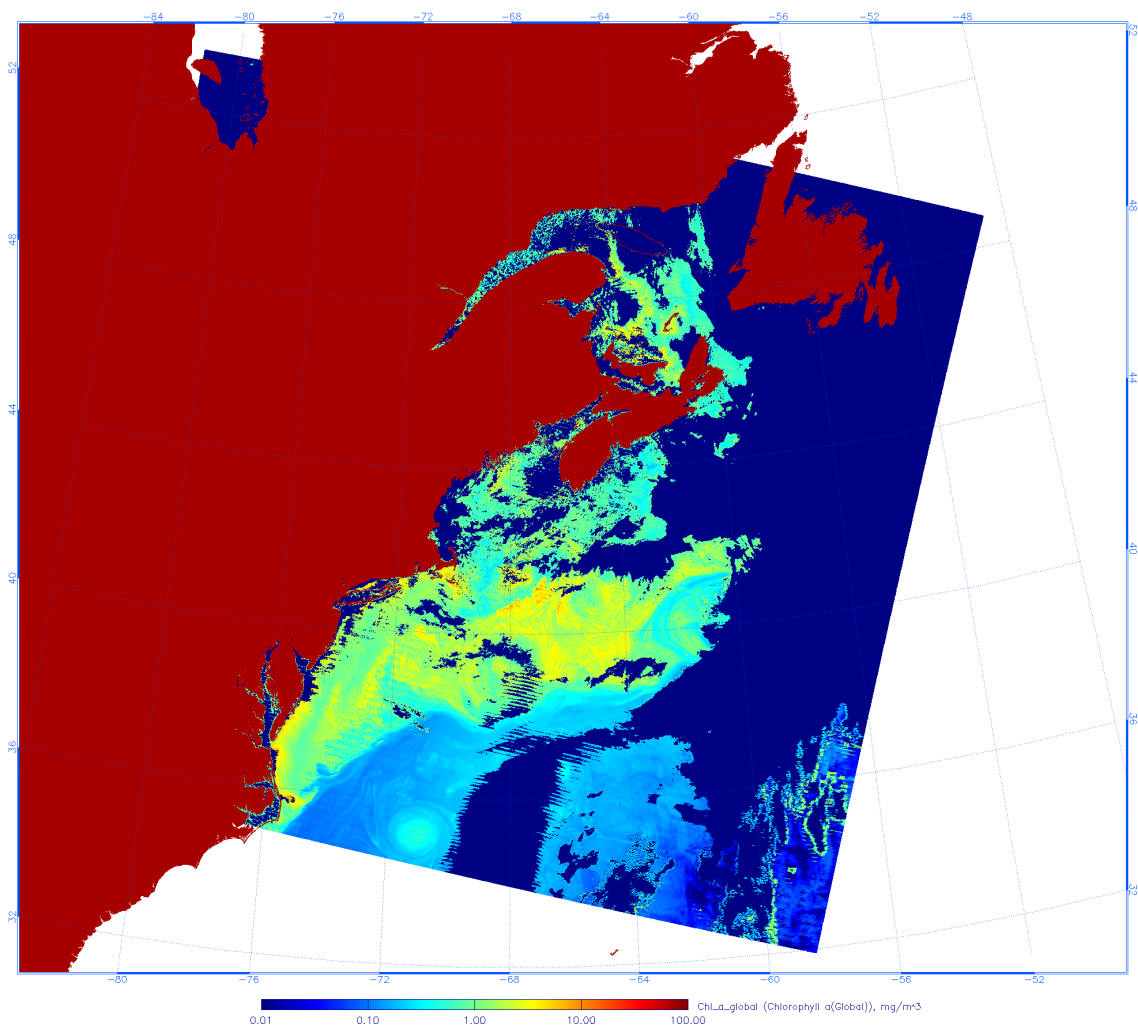


**Figure 7 Chlorophyll *a* concentrations derived using the Carder et al. (1999) algorithm with MODIS water-leaving radiance values, obtained using a fixed, global parameterization of the package effect (pk=0; see Fig. 5) rather than using four different domains.**

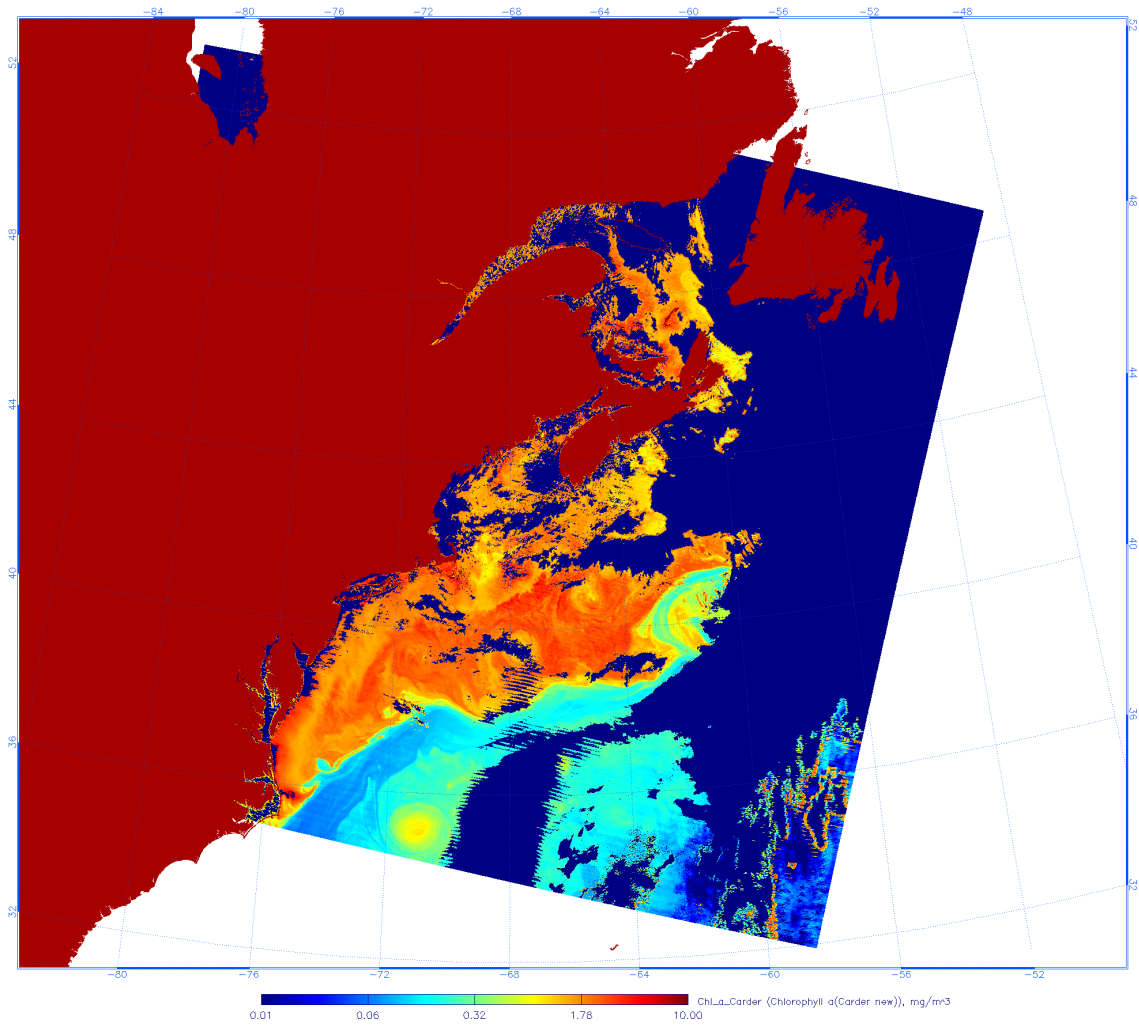


**Figure 8 Chlorophyll *a* concentrations derived using the Carder et al. (1999) algorithm with MODIS water-leaving radiance values, obtained using the four different domains with smooth transitions as shown in Figure 5.**

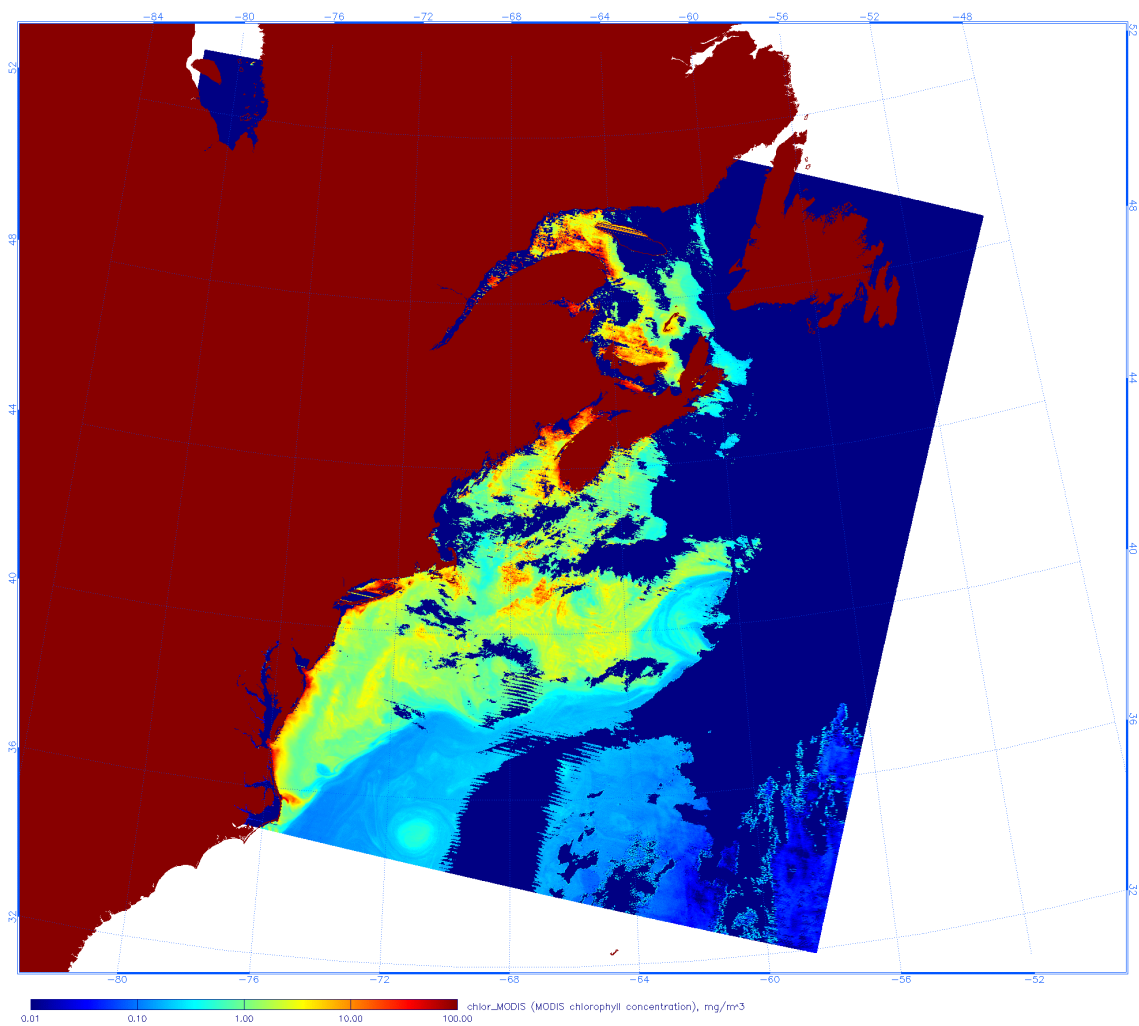


**Figure 9 Chlorophyll *a* concentrations derived using the Chlor\_MODIS band-ratio algorithm with MODIS water-leaving radiance values.**

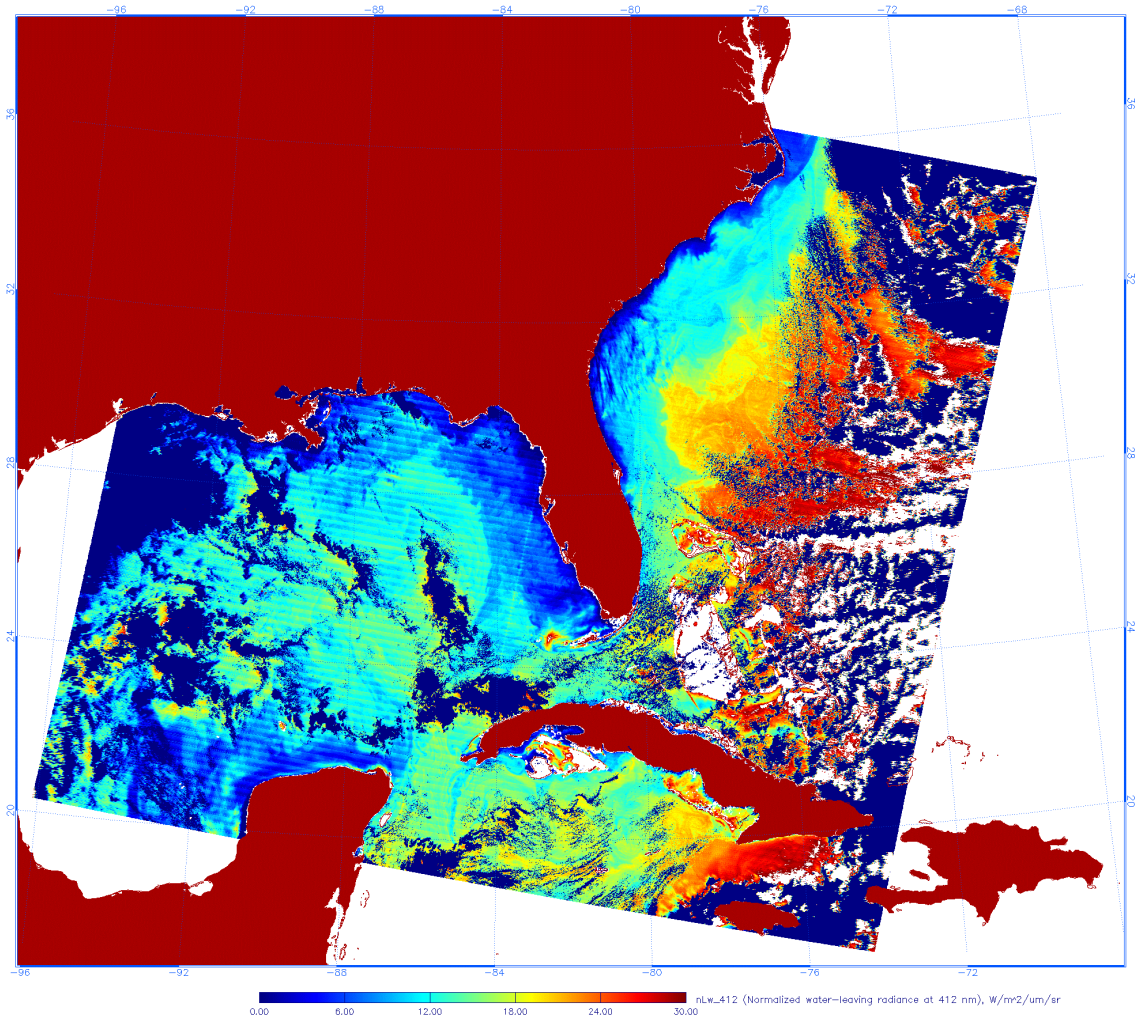


**Figure 10a Normalized water-leaving radiance values at 412 nm for the Gulf of Mexico on Julian Day 306 2000. Note the most severe striping occurs on the west sides of the image.**

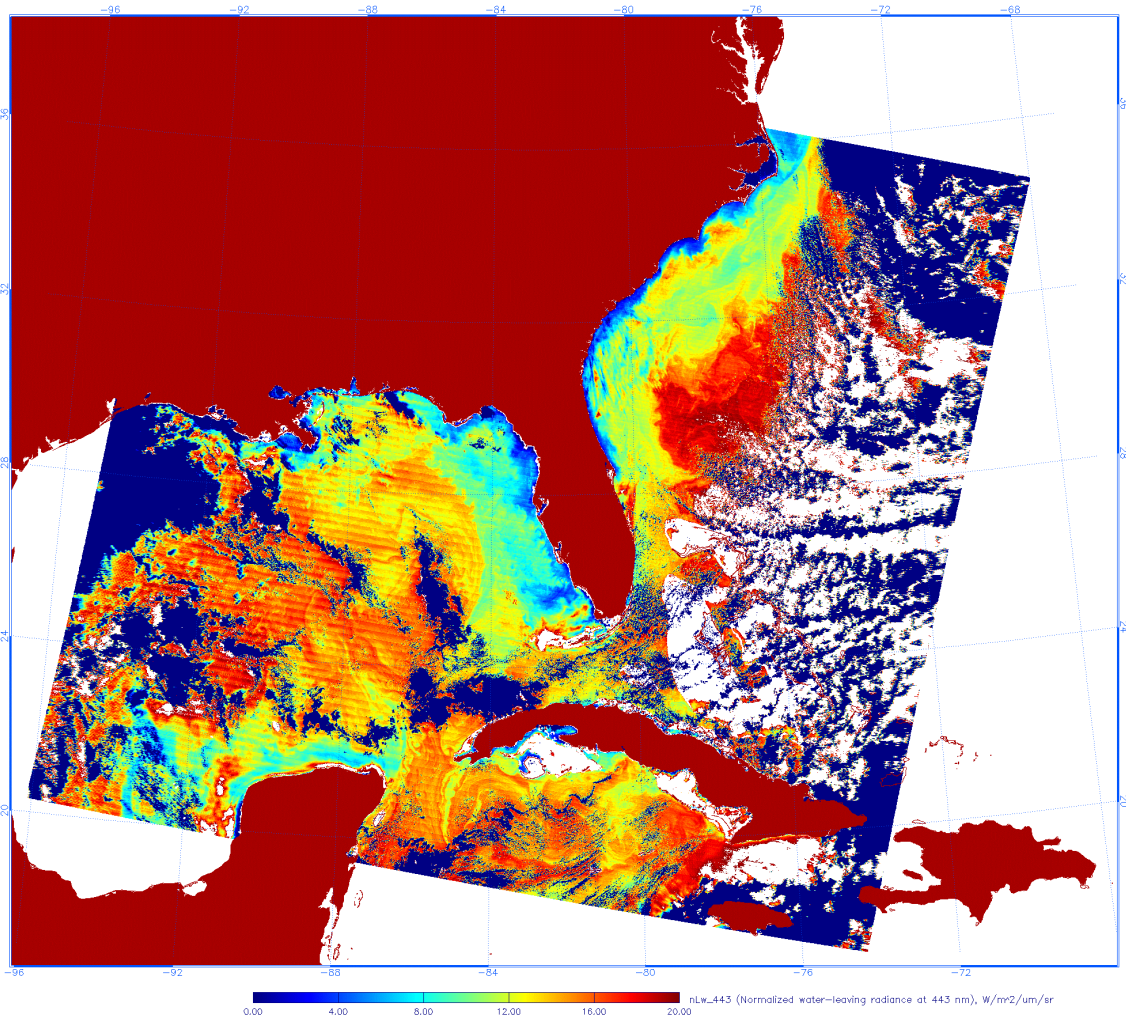


**Figure 10b Normalized water-leaving radiance values at 443 nm for the Gulf of Mexico on Julian Day 306 2000. Note the most severe striping occurs on the west sides of the image.**